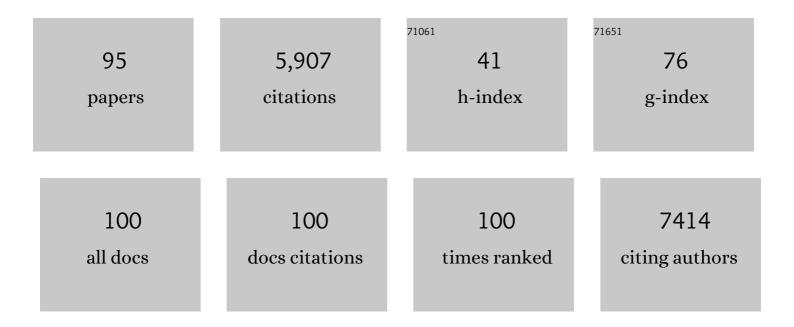
Roger Wepf

List of Publications by Year in descending order

Source: https://exaly.com/author-pdf/8235922/publications.pdf Version: 2024-02-01



ROCED WEDE

#	Article	IF	CITATIONS
1	Ptychographic X-ray computed tomography at the nanoscale. Nature, 2010, 467, 436-439.	13.7	766
2	Nanoparticles – An efficient carrier for drug delivery into the hair follicles. European Journal of Pharmaceutics and Biopharmaceutics, 2007, 66, 159-164.	2.0	488
3	Distribution of sunscreens on skin. Advanced Drug Delivery Reviews, 2002, 54, S157-S163.	6.6	250
4	Rab8 promotes polarized membrane transport through reorganization of actin and microtubules in fibroblasts Journal of Cell Biology, 1996, 135, 153-167.	2.3	228
5	Direct observation of individual hydrogen atoms at trapping sites in a ferritic steel. Science, 2017, 355, 1196-1199.	6.0	224
6	Roles for Rac1 and Cdc42 in planar polarization and hair outgrowth in the wing of Drosophila Journal of Cell Biology, 1996, 135, 1277-1289.	2.3	203
7	3D geometry and topology of pore pathways in Opalinus clay: Implications for mass transport. Applied Clay Science, 2011, 52, 85-95.	2.6	190
8	Phase tomography from x-ray coherent diffractive imaging projections. Optics Express, 2011, 19, 21345.	1.7	183
9	Entry of the Two Infectious Forms of Vaccinia Virus at the Plasma Membane Is Signaling-Dependent for the IMV but Not the EEV. Molecular Biology of the Cell, 2000, 11, 2497-2511.	0.9	162
10	Measuring single-nanoparticle wetting properties by freeze-fracture shadow-casting cryo-scanning electron microscopy. Nature Communications, 2011, 2, 438.	5.8	159
11	The Human Stratum corneum Layer: An Effective Barrier against Dermal Uptake of Different Forms of Topically Applied Micronised Titanium Dioxide. Skin Pharmacology and Physiology, 2001, 14, 92-97.	1.1	143
12	A novel nuclear pore protein Nup133p with distinct roles in poly(A)+ RNA transport and nuclear pore distribution. EMBO Journal, 1994, 13, 6062-75.	3.5	143
13	Towards quantitative 3D imaging of the osteocyte lacuno-canalicular network. Bone, 2010, 47, 848-858.	1.4	139
14	Serial FIB/SEM imaging for quantitative 3D assessment of the osteocyte lacuno-canalicular network. Bone, 2011, 49, 304-311.	1.4	123
15	The Mechanism of Toxicity in HET-S/HET-s Prion Incompatibility. PLoS Biology, 2012, 10, e1001451.	2.6	123
16	The Largest Synthetic Structure with Molecular Precision: Towards a Molecular Object. Angewandte Chemie - International Edition, 2011, 50, 737-740.	7.2	111
17	The core of the mammalian centriole contains Î ³ -tubulin. Current Biology, 1995, 5, 1384-1393.	1.8	110
18	Nic96p is required for nuclear pore formation and functionally interacts with a novel nucleoporin, Nup188p Journal of Cell Biology, 1996, 133, 1141-1152.	2.3	99

#	Article	IF	CITATIONS
19	Simultaneous Correlative Scanning Electron and High-NA Fluorescence Microscopy. PLoS ONE, 2013, 8, e55707.	1.1	95
20	Dead but Highly Dynamic – The Stratum corneum Is Divided into Three Hydration Zones. Skin Pharmacology and Physiology, 2004, 17, 246-257.	1.1	91
21	3D-microstructure analysis of hydrated bentonite with cryo-stabilized pore water. Applied Clay Science, 2010, 47, 330-342.	2.6	84
22	On the application of focused ion beam nanotomography in characterizing the 3D pore space geometry of Opalinus clay. Physics and Chemistry of the Earth, 2011, 36, 1539-1544.	1.2	75
23	From tissue to cellular ultrastructure: closing the gap between micro- and nanostructural imaging. Journal of Microscopy, 2003, 212, 91-99.	0.8	72
24	Three-dimensional mass density mapping of cellular ultrastructure by ptychographic X-ray nanotomography. Journal of Structural Biology, 2015, 192, 461-469.	1.3	72
25	Sealing the live part of the skin: The integrated meshwork of desmosomes, tight junctions and curvilinear ridge structures in the cells of the uppermost granular layer of the human epidermis. European Journal of Cell Biology, 2004, 83, 655-665.	1.6	71
26	Robust workflow and instrumentation for cryo-focused ion beam milling of samples for electron cryotomography. Ultramicroscopy, 2018, 190, 1-11.	0.8	68
27	Localization of Ceramide and Glucosylceramide in Human Epidermis by Immunogold Electron Microscopy. Journal of Investigative Dermatology, 2001, 117, 1126-1136.	0.3	67
28	Mechanisms of haptoglobin protection against hemoglobin peroxidation triggered endothelial damage. Cell Death and Differentiation, 2013, 20, 1569-1579.	5.0	65
29	High-Pressure Freezing Provides New Information on Human Epidermis: Simultaneous Protein Antigen and Lamellar Lipid Structure Preservation. Study on Human Epidermis by Cryoimmobilization. Journal of Investigative Dermatology, 2000, 114, 1030-1038.	0.3	62
30	Bridging Microscopes. Methods in Cell Biology, 2012, 111, 325-356.	0.5	62
31	Risk estimation of skin damage due to ultrashort pulsed, focused near-infrared laser irradiation at 800â€,nm. Journal of Biomedical Optics, 2008, 13, 041320.	1.4	57
32	Structure and Assembly of Intracellular Mature Vaccinia Virus: Isolated-Particle Analysis. Journal of Virology, 2001, 75, 11034-11055.	1.5	55
33	Cryoâ€FIBâ€nanotomography for quantitative analysis of particle structures in cement suspensions. Journal of Microscopy, 2007, 227, 216-228.	0.8	54
34	Threeâ€dimensional pore structure and ion conductivity of porous ceramic diaphragms. AICHE Journal, 2013, 59, 1446-1457.	1.8	52
35	Assessing the risk of skin damage due to femtosecond laser irradiation. Journal of Biophotonics, 2008, 1, 470-477.	1.1	50
36	Platinum/iridium/carbon: a highâ€resolution shadowing material for TEM, STM and SEM of biological macromolecular structures. Journal of Microscopy, 1991, 163, 51-64.	0.8	49

#	Article	IF	CITATIONS
37	OMNY—A tOMography Nano crYo stage. Review of Scientific Instruments, 2018, 89, 043706.	0.6	48
38	Are Sweat Glands an Alternate Penetration Pathway? Understanding the Morphological Complexity of the Axillary Sweat Gland Apparatus. Skin Pharmacology and Physiology, 2006, 19, 38-49.	1.1	47
39	Height and Width of Adsorbed Dendronized Polymers: Electron and Atomic Force Microscopy of Homologous Series. Macromolecules, 2011, 44, 6785-6792.	2.2	46
40	Investigation of differences in follicular penetration of particle-and nonparticle-containing emulsions by laser scanning microscopy. Laser Physics, 2006, 16, 747-750.	0.6	44
41	OMNY PIN—A versatile sample holder for tomographic measurements at room and cryogenic temperatures. Review of Scientific Instruments, 2017, 88, 113701.	0.6	44
42	In Situ Techniques for Developing Robust Li–S Batteries. Small Methods, 2018, 2, 1800133.	4.6	41
43	Mouse anti-ceramide antiserum: a specific tool for the detection of endogenous ceramide. Glycobiology, 2001, 11, 451-457.	1.3	40
44	Investigation of the swelling of human skin cells in liquid media by tapping mode scanning force microscopy. Applied Physics A: Materials Science and Processing, 2001, 72, S125-S128.	1.1	39
45	Freezing Continuous-Flow Self-Assembly in a Microfluidic Device: Toward Imaging of Liposome Formation. Langmuir, 2013, 29, 1717-1723.	1.6	37
46	Characterization of Catalysts in an Aberration-Corrected Scanning Transmission Electron Microscope. Journal of Physical Chemistry C, 2011, 115, 1080-1083.	1.5	33
47	Penetration pathways of fluorescent dyes in human hair fibres investigated by scanning near-field optical microscopy. Journal of Microscopy, 2000, 200, 179-186.	0.8	27
48	Title is missing!. International Journal of Cosmetic Science, 1999, 21, 399-411.	1.2	25
49	Focussed ion beam nanotomography reveals the 3D morphology of different solid phases in hardened cement pastes. Journal of Microscopy, 2011, 241, 234-242.	0.8	24
50	Minimization of amorphous layer in Ar+ ion milling for UHR-EM. Ultramicroscopy, 2011, 111, 1224-1232.	0.8	23
51	Methods in Creating, Transferring, & Measuring Cryogenic Samples for APT. Microscopy and Microanalysis, 2015, 21, 517-518.	0.2	23
52	STM of freeze-dried and Ptî—,Irî—,C-coated bacteriophage T4 polyheads. Journal of Structural Biology, 1989, 102, 170-177.	0.9	22
53	Influence of pH on colloidal properties and surface activity of polyglycerol fatty acid ester vesicles. Journal of Colloid and Interface Science, 2008, 327, 446-450.	5.0	22
54	Pros and cons: cryo-electron microscopic evaluation of block faces versus cryo-sections from frozen-hydrated skin specimens prepared by different techniques. Journal of Microscopy, 2007, 225, 201-207.	0.8	21

#	Article	IF	CITATIONS
55	Phase-contrast imaging in aberration-corrected scanning transmission electron microscopy. Micron, 2013, 49, 1-14.	1.1	19
56	Hydration dynamics of human fingernails: An ellipsometric study. Physical Review E, 2002, 65, 061913.	0.8	17
57	Correlative 3D Imaging: CLSM and FIB-SEM Tomography Using High-Pressure Frozen, Freeze-Substituted Biological Samples. Methods in Molecular Biology, 2014, 1117, 593-616.	0.4	16
58	A strategy for correlative microscopy of large skin samples: towards a holistic view of axillary skin complexity. Experimental Dermatology, 2008, 17, 73-81.	1.4	14
59	The ultrastructure of fibronectin fibers pulled from a protein monolayer at the air-liquid interface and the mechanism of the sheet-to-fiber transition. Biomaterials, 2015, 36, 66-79.	5.7	14
60	Noninvasive measurement of cell volume changes by negative staining. Journal of Biomedical Optics, 2005, 10, 064017.	1.4	13
61	Threeâ€dimensional reconstruction of biological macromolecular complexes from inâ€lens scanning electron micrographs. Journal of Microscopy, 2009, 234, 287-292.	0.8	13
62	A Versatile High-Vacuum Cryo-transfer System for Cryo-microscopy and Analytics. Biophysical Journal, 2016, 110, 758-765.	0.2	13
63	TEM moiré patterns explain STM images of bacteriophage T5 tails. Ultramicroscopy, 1997, 69, 129-137.	0.8	12
64	Three-dimensional reconstruction of Heterocapsa circularisquama RNA virus by electron cryo-microscopy. Journal of General Virology, 2011, 92, 1960-1970.	1.3	12
65	Enabling Atom Probe Analyses of New Materials Classes with Vacuum-Cryo-Transfer Capabilities. Microscopy and Microanalysis, 2017, 23, 612-613.	0.2	11
66	A Versatile High-Vacuum Cryo-Transfer for Cryo-FESEM, Cryo-SPM and other Imaging Techniques. Microscopy and Microanalysis, 1999, 5, 424-425.	0.2	8
67	Correlation of live-cell imaging with volume scanning electron microscopy. Methods in Cell Biology, 2017, 140, 123-148.	0.5	8
68	Improvements for HR- and Cryo-SEM by the VCT 100 High-Vacuum Cryo Transfer System and SEM Cooling Stage. Microscopy and Microanalysis, 2004, 10, 970-971.	0.2	6
69	Surface layer of Ptâ€Oâ€Ce bonds on CeO x nanowire with high ORR activity converted by proton beam irradiation. Journal of the American Ceramic Society, 2021, 104, 1945-1952.	1.9	6
70	Skin imaged by femtosecond laser irradiation: a risk assessment for in vivo applications. , 2006, 6191, 36.		5
71	Topographic Measurements of Real Structures in reflection Confocal Laser Scanning Microscope (CLSM). Microscopy and Microanalysis, 2003, 9, 162-163.	0.2	4
72	Correlative 3D Microscopy: CLSM and FIB/SEM Tomography. Imaging & Microscopy, 2008, 10, 30-31.	0.1	4

#	Article	IF	CITATIONS
73	Visualizing nuclei in skin cryosections: viable options to 46-diamidino-2-phenylindol for confocal laser microscopy. Skin Research and Technology, 2008, 14, 324-326.	0.8	4
74	Macromolecular 3D SEM reconstruction strategies: Signal to noise ratio and resolution. Ultramicroscopy, 2014, 144, 43-49.	0.8	4
75	Correlative UHV-Cryo Transfer Suite: Connecting Atom Probe, SEM-FIB, Transmission Electron Microscopy via an Environmentally-Controlled Glovebox. Microscopy and Microanalysis, 2019, 25, 2494-2495.	0.2	4
76	Quantification of total calcium in terminal cisternae of skinned muscle fibers by imaging electron energy-loss spectroscopy. Journal of Muscle Research and Cell Motility, 1999, 20, 505-515.	0.9	3
77	Characterization of multiphoton laser scanning device optical parameters for image restoration. , 2004, , .		3
78	Structural investigations of human hairs by spectrally resolved ellipsometry. Journal of Biomedical Optics, 2006, 11, 014029.	1.4	3
79	The structure of dodecagonal (Ta,V)1.6Te imaged by phase-contrast scanning transmission electron microscopy. Journal of Solid State Chemistry, 2012, 194, 106-112.	1.4	3
80	A cryogenic scanning force microscope for the characterization of frozen biological samples. Applied Physics A: Materials Science and Processing, 2003, 76, 893-898.	1.1	2
81	Addendum to "Three-dimensional mass density mapping of cellular ultrastructure by ptychographic X-ray nanotomography―[J. Struct. Biol. 192 (2015) 461–469]. Journal of Structural Biology, 2016, 193, 83.	1.3	2
82	ENZEL - A cryogenic, retrofittable, coincident fluorescence, electron, and ion beam solution for the cryo-electron tomography workflow Microscopy and Microanalysis, 2021, 27, 3228-3229.	0.2	2
83	Correlative 3D microscopy: CLSM and FIB/SEM tomography used to study cellular entry of vaccinia virus. , 2008, , 361-362.		2
84	Active Pt-Nanocoated Layer with Pt–O–Ce Bonds on a CeO _{<i>x</i>} Nanowire Cathode Formed by Electron Beam Irradiation. ACS Omega, 0, , .	1.6	2
85	Cryopreparation of skin samples: A comparison between ultrathin cryosections and resin embedded sections of human skin. Microscopy and Microanalysis, 2003, 9, 180-181.	0.2	1
86	Fluorescence-guided lamella fabrication with ENZEL, an integrated cryogenic CLEM solution for the cryo-electron tomography workflow. Microscopy and Microanalysis, 2021, 27, 3234-3235.	0.2	1
87	Publisher's Note: Hydration dynamics of human fingernails: An ellipsometric study [Phys. Rev. E65, 061913 (2002)]. Physical Review E, 2002, 66, .	0.8	0
88	No compromise in correlative microscopy: One sample, one preparation protocol for CLSM and TEM. Microscopy and Microanalysis, 2003, 9, 1198-1199.	0.2	0
89	Combining histological and ultrastructural description of high-pressure frozen skin samples by correlative CLSM and TEM. Microscopy and Microanalysis, 2003, 9, 374-375.	0.2	0
90	Improving image storage and access in an integrated microscopy unit: experiences with a commercial image database system. Microscopy and Microanalysis, 2003, 9, 530-531.	0.2	0

#	Article	IF	CITATIONS
91	Improved Native Tissue Ultrastructure Investigations by High Pressure Freezing and Cryo-SEM. Microscopy and Microanalysis, 2006, 12, 1114-1115.	0.2	0
92	Life-Like Physical Fixation of Large Samples for Correlative Microscopy. Microscopy and Microanalysis, 2008, 14, 680-681.	0.2	0
93	Can one determine the density of an individual synthetic macromolecule?. Soft Matter, 2019, 15, 6547-6556.	1.2	0
94	The Surface Structure of Biomolecules Using Correlative Microscopy: TEM, SEM, STM and AFM. Proceedings Annual Meeting Electron Microscopy Society of America, 1996, 54, 314-315.	0.0	0
95	Life-like physical fixation of large samples for correlative microscopy. , 2008, , 351-352.		0